VASCULAR – Whole-Body Angiography

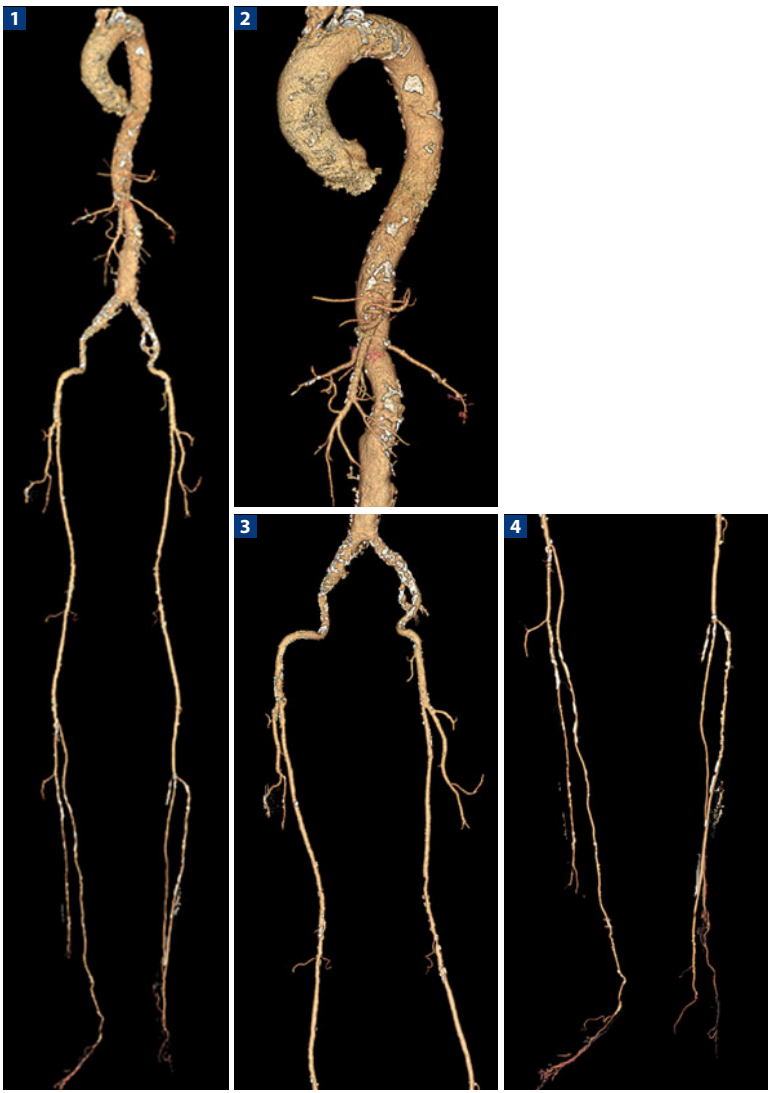

Images reconstructed with a VR algorithm of a whole-body angiography study in a diabetic patient. **1** Note the excellent representation of the entire aorta, the mesenteric vessels, and the vascular regions of the lower limbs and the feet. **2** Detail of the thoraco-abdominal aorta and the mesenteric vessels. Note the diffuse parietal calcifications. **3** Detail of the iliac-femoral region. **4** Detail of the distal run-off and the circulation of the feet

A. Laghi (ed.), *MDCT Protocols*, © Springer-Verlag 2012

Study Protocol

Patient preparation: A 6-h fast prior to the examination; 18G intravenous catheter in the right antecubital vein and 1.2 gl/s.

Iodine flow rate: 2.0 gl/s and 1.2 gl/s.

CM concentration (mgl/mL)	Flow rate (mL/s)
300	6.7/4
320	6.2/3.7
350	5.7/3.4
370	5.4/3.2
400	5.0/3

Pre-contrast scan: Unnecessary.

Post-contrast scan:
CM injection protocol:
Fixed injection time: 35 s (for patients between 60 and 90 kg).
Biphasic protocol: 1/3 of CM at 2 gl/s followed by 2/3 of CM at 1.2 gl/s every s after the threshold of 100 HU is reached in the ascending aorta using a bolus-tracking technique.
Saline flush: 50 ml of saline at the same flow rate.
Scan protocol: An arterial phase is mandatory. The diagnostic protocol provides lower kV values (80–100 kV) with fixed mA (200 mA); alternatively, automated techniques to reduce mA can be used.
Scan region: From the aortic arch to the foot.

References

Jackowski C, Persson A, Thali MJ et al (2008) Whole body postmortem angiography with a high viscosity contrast agent solution using poly ethylene glycol as contrast agent dissolver. J Forensic Sci 53:465-468

Napoli A, Anzidei M, Francone M et al (2008) 64-MDCT imaging of the coronary arteries and systemic arterial vascular tree in a single examination: optimisation of the scan protocol and contrast-agent administration. Radiol Med 113:799-816

Ross S, Spendlove D, Bolliger S et al (2008) Postmortem whole-body CT angiography: evaluation of two contrast media solutions. AJR Am J Roentgenol 190:1380-1389

VASCULAR – Carotid Arteries-Carotid Stenosis with Ulcerated Plaque

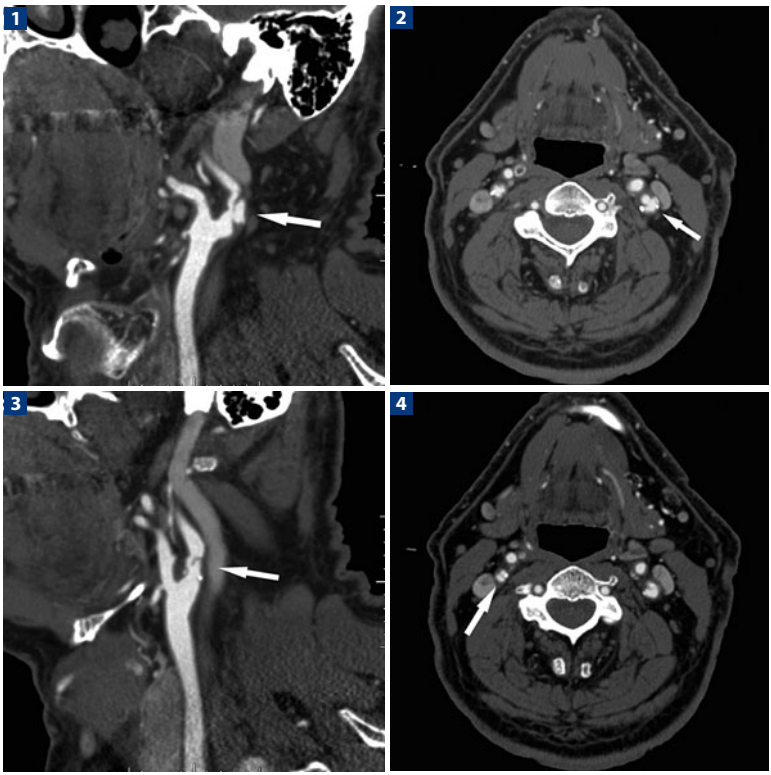

Patient with bilateral carotid stenosis. **1** Sagittal reformation image shows an ulcerated fibrotic plaque of the left internal carotid artery (*arrow*). **2** Stenosis of the left internal carotid artery by a fibrotic plaque with extensive ulceration (*arrow*) is seen in this axial image. **3** Sagittal reformation image reveals a partial intimal dissection at the level of the internal carotid artery (*arrow*). **4** Axial image shows partial intimal dissection (*arrow*)

Study Protocol

Patient preparation: A 6-h fast pior to the examination; 18G intravenous catheter in the right antecubital vein.

Iodine flow rate: 2.0 gI/s.

CM concentration (mgI/mL)	Flow rate (mL/s)
300	6.7
320	6.2
350	5.7
370	5.4
400	5.0

CM volume: (Scan time + trigger delay)*flow rate.

Saline flush: 50 ml of saline at the same flow rate.

Pre-contrast scan: Unnecessary.

Post-contrast scan:
CM injection protocol: Injection time = scan time + 3-s delay.
Diagnostic delay: 3 s after the value of 100 HU is reached, with the ROI in the ascending thoracic aorta.
Scan protocol: Spiral, caudate-cranial with maximum values of pitch and thin collimation.
Scan region: From the aortic arch to the skull base.

References

Forsting M (2005) CTA of the ICA bifurcation and intracranial vessels. Eur Radiol 15 Suppl 4:D25-D27

Koelemay MJ, Nederkoorn PJ, Reitsma JB et al (2004) Systematic review of computed tomographic angiography for assessment of carotid artery disease. Stroke 35:2306-2312

Saba L, Sanfilippo R, Pirisi R et al (2007) Multidetector-row CT angiography in the study of atherosclerotic carotid arteries. Neuroradiology 49:623-637

VASCULAR – Evaluation of Carotid Stent

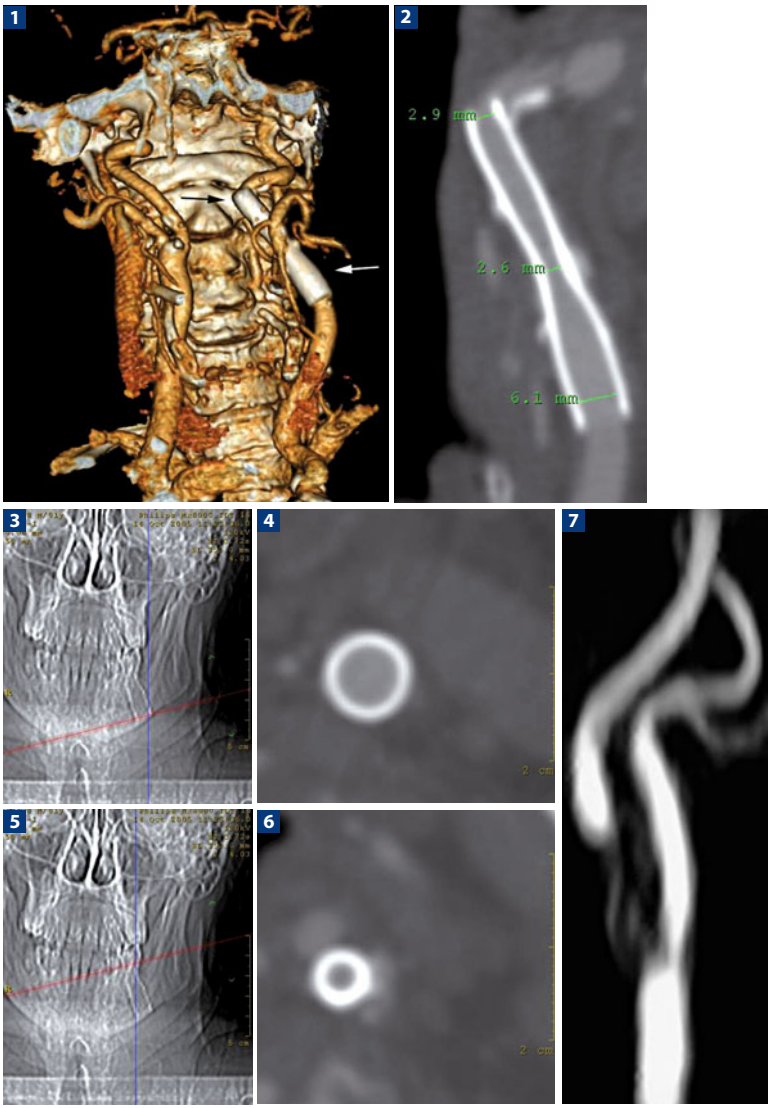

1 The stent is evident in volumetric images (*arrow*), which do not provide information about its patency. **2** Data obtained through the analysis of longitudinal axial-oblique reconstructions of the stent axis. **3-6** The condition of the stent is seen on the anterior-posterior scanogram. **7** No information was obtained from the angio-MRI study with gadolinium

Study Protocol

Patient preparation: A 6-h fast pior to the examination; 18G intravenous catheter in the right antecubital vein.

Iodine flow rate: 2.0 gI/s.

CM concentration (mgI/mL)	Flow rate (mL/s)
300	6.7
320	6.2
350	5.7
370	5.4
400	5.0

CM volume: (Scan time + trigger delay)*flow rate.

Saline flush: 50 ml of saline at the same flow rate.

Pre-contrast scan: Unnecessary.

Post-contrast scan:
CM injection protocol: Injection time = scan time + 3-s delay.
Diagnostic delay: 3 s after the value of 100 HU is reached, with the ROI in the ascending thoracic aorta.
Scan protocol: Spiral, caudate-cranial with maximum values of pitch and thin collimation.
Scan region: From the aortic arch to the skull base.

References

Kwon BJ, Jung C, Sheen SH et al (2007) CT angiography of stented carotid arteries: comparison with Doppler ultrasonography. J Endovasc Ther 14:489-497

Orbach DB, Pramanik BK, Lee J et al (2006) Carotid artery stent implantation: evaluation with multi-detector row CT angiography and virtual angioscopy-initial experience. Radiology 238:309-320

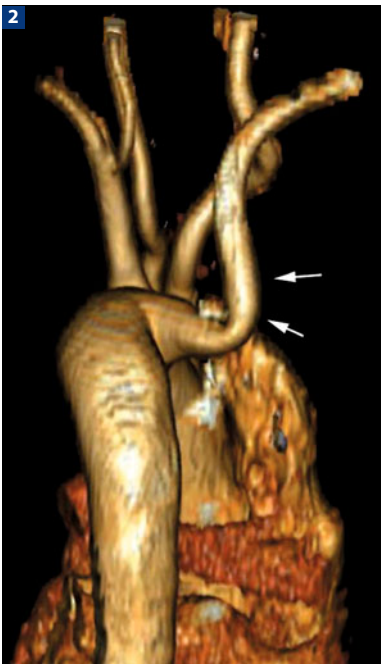

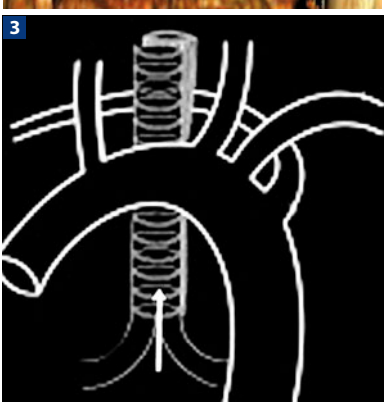

1, **2** Anatomical variation consisting of a direct origin of the right subclavian artery which has a retro-esophageal course (lusory artery). The schema is shown in **3**. The patient was asymptomatic; the anomaly was observed during a chest CT

Study Protocol

Patient preparation: A 6-h fast prior to the examination; 18G intravenous catheter in the right antecubital vein.

Iodine flow rate: 2.0 gI/s.

CM concentration (mgI/mL)	Flow rate (mL/s)
300	6.7
320	6.2
350	5.7
370	5.4
400	5.0

CM volume: (Scan time + trigger delay)*flow rate.

Saline flush: 50 ml of saline at the same flow rate.

Pre-contrast scan: Unnecessary.

Post-contrast scan:
CM injection protocol: Injection time = scan time + 7-s trigger delay.
Trigger delay: 7s after the threshold of 100 HU is reached in the ascending aorta using a bolus-tracking technique.
Scan protocol:
Scan region: From the aortic arch to the heart apex.
Spiral with maximum values of pitch and thin collimation.

References

Dursun M, Yilmaz S, Sayin OA et al (2007) Combination of unicuspid aortic valve, aortic coarctation, and aberrant right subclavian artery in a child: MR imaging and CTA findings. Cardiovasc Intervent Radiol 30:547-549

VASCULAR – Post-traumatic Thoracic Aorta Aneurysm (with Cardiac Gating)

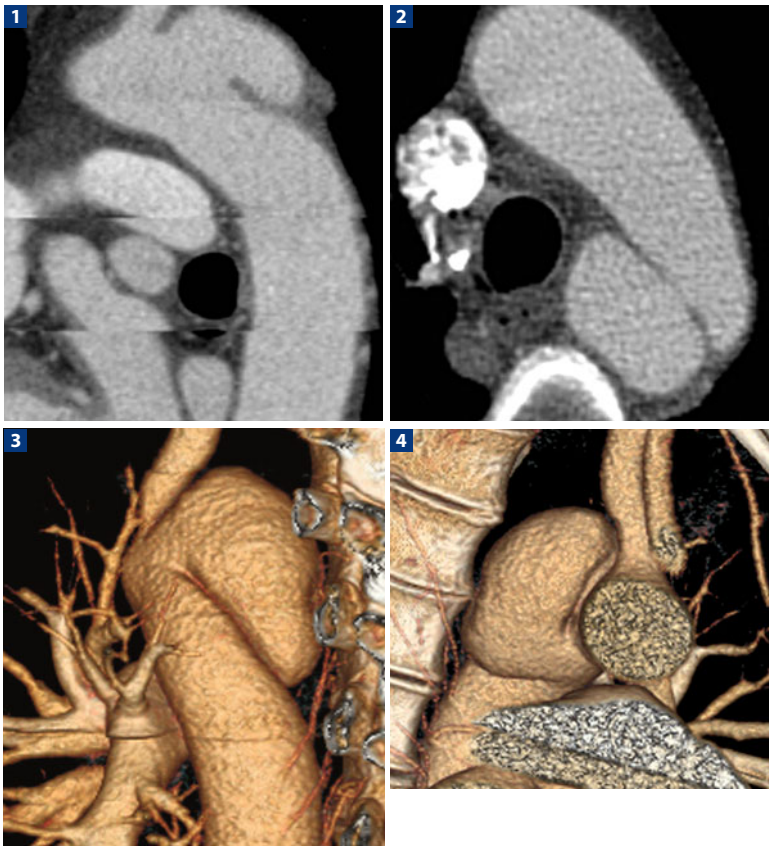

Post-traumatic pseudoaneurysm at the level of the isthmus, the area of the aorta most frequently involved by traumatic lesions. In this study of the thoracic aorta with cardiac gating, note the presence of artifacts produced by ectopic heart beats. **1** Sagittal MIP reconstruction. **2** The 2D axial image shows a detail of the neck of the pseudoaneurysm. Note the close relation with the esophageal wall, a risk factor for possible fistula formation. **3** VR reconstruction identifies the pseudoaneurysm, highlighting its atypical morphology, which is quite different from the saccular or spindle-like morphology of true aneurysms. **4** VR reconstruction shows the aneurysm and its anatomical relations

Study Protocol

Patient preparation: A 6-h fast prior to the examination; 18G intravenous catheter in the right antecubital vein.

Iodine flow rate: 2.0 gI/s.

CM concentration (mgI/mL)	Flow rate (mL/s)
300	6.7
320	6.2
350	5.7
370	5.4
400	5.0

CM volume: (Scan time + trigger delay)*flow rate.

Saline flush: 50 ml of saline at the same flow rate.

Pre-contrast scan: Unnecessary.

Post-contrast scan:
CM injection protocol: Injection time = scan time + 7-s trigger delay.
Trigger delay: 7 s after the threshold of 100 HU is reached in the ascending aorta using a bolus-tracking technique.
Scan protocol:
Gating: Retrospective or prospective (according to patient HR and technology available).
Scan region: From the aortic arch to the heart apex.

References

Ledbetter S, Stuk JL, Kaufman JA et al (1999) Helical (spiral) CT in the evaluation of emergent thoracic aortic syndromes. Traumatic aortic rupture, aortic aneurysm, aortic dissection, intramural hematoma, and penetrating atherosclerotic ulcer. Radiol Clin North Am 37:575-589

Manghat NE, Morgan-Hughes GJ, Roobottom CA et al (2005) Multi-detector row computed tomography: imaging in acute aortic syndrome. Clin Radiol 60:1256-1267

Salvolini L, Renda P, Fiore D et al (2008) Acute aortic syndromes: role of multidetector row CT. Eur J Radiol 65:350-358

VASCULAR – Perforating Ulcer of the Thoracic Aorta (without Cardiac Gating)

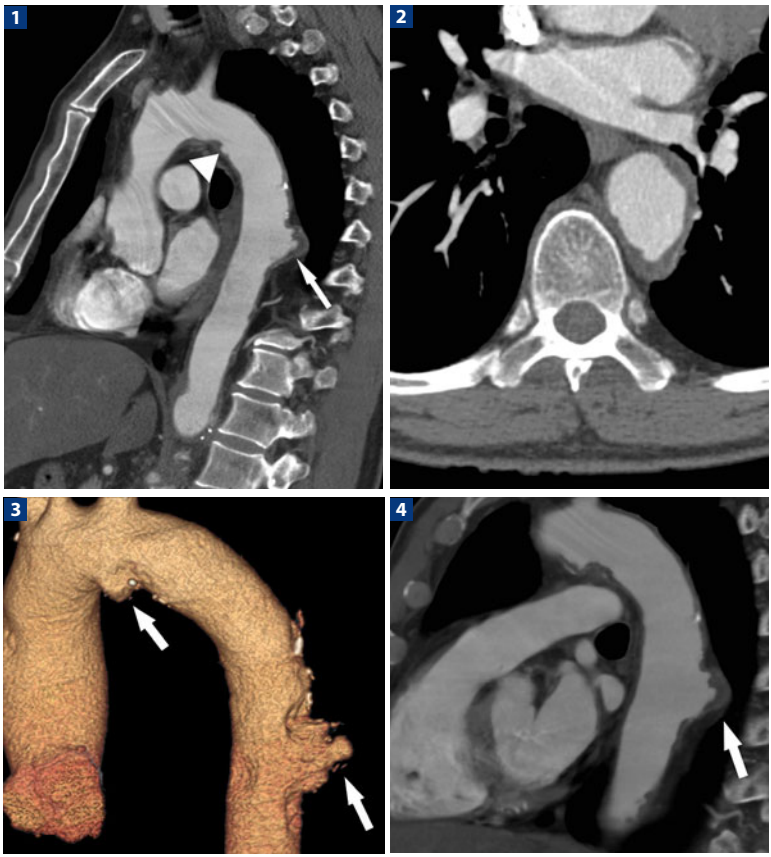

Study of the thoracic aorta without cardiac gating. **1** Sagittal MPR image shows a large perforating ulcer of the posterior wall of the thoracic aorta (*arrow*) and a small ulcer of the inferior wall of the aortic arch (*arrowhead*). **2** The 2D axial image shows a detail of the perforating ulcer of the thoracic aorta. Note the thrombotic apposition within the ulcer itself. **3** VR reconstruction demonstrates the spindle-shaped aneurysm of the ascending aorta and the two "plus" images (*arrows*) corresponding to the two parietal ulcers. **4** Oblique MIP reconstruction shows the perforating ulcer of the thoracic aorta, highlighting its marked retro-aortic extension

Study Protocol

Patient preparation: A 6-h fast prior to the examination; 18G intravenous catheter in the right antecubital vein.

Iodine flow rate: 2.0 gI/s.

CM concentration (mgI/mL)	Flow rate (mL/s)
300	6.7
320	6.2
350	5.7
370	5.4
400	5.0

CM volume: (Scan time + trigger delay)*flow rate.

Saline flush: 50 ml of saline at the same flow rate.

Pre-contrast scan: Unnecessary.

Post-contrast scan:
CM injection protocol: Injection time = scan time + 7-s trigger delay.
Trigger delay: 7s after the threshold of 100 HU is reached in the ascending aorta using a bolus-tracking technique.
Scan protocol:
Scan region: From the aortic arch to the heart apex.
Spiral with maximum values of pitch and thin collimation.

References

Hayashi H, Matsuoka Y, Sakamoto I et al (2000) Penetrating atherosclerotic ulcer of the aorta: imaging features and disease concept. RadioGraphics 20:995-1005

Johnson TR, Nikolaou K, Wintersperger BJ et al (2007) Optimization of contrast material administration for electrocardiogram-gated computed tomographic angiography of the chest. J Comput Assist Tomogr 31:265-271

Takahashi K, Stanford W (2005) Multidetector CT of the thoracic aorta. Int J Cardiovasc Imaging 21:141-153

VASCULAR – Aortic Dissection Type A

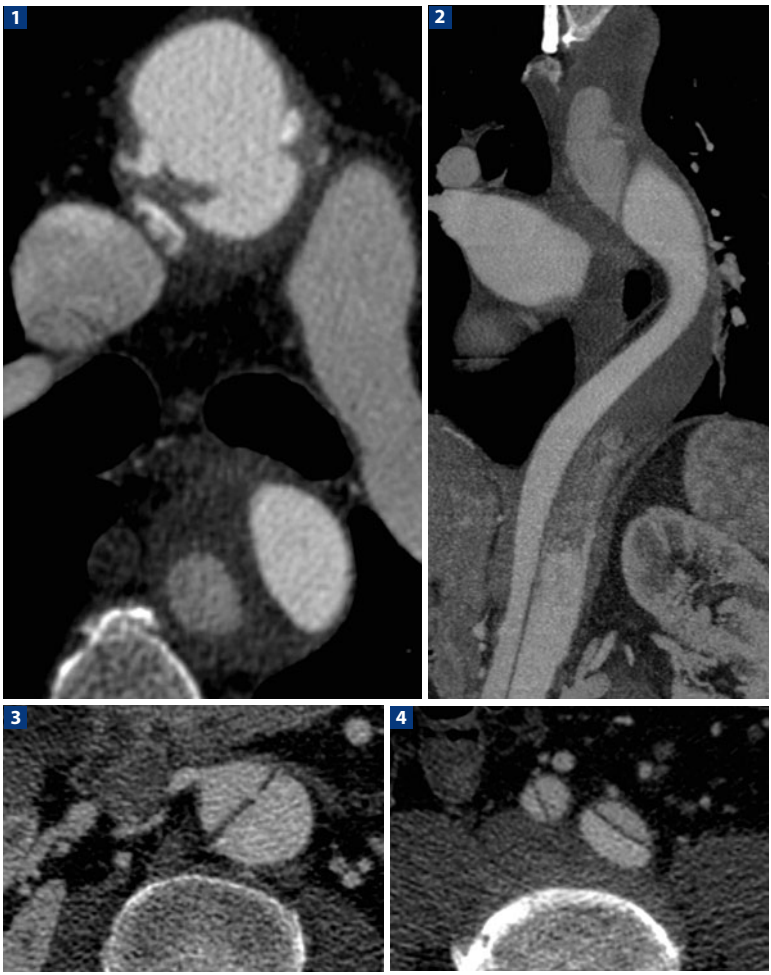

1 Two-dimensional axial image shows the dissection arising at the level of the ascending aorta and the double lumen at the level of the descending thoracic aorta, with less enhancement of the false lumen. **2** On oblique MPR image, the dissection can be seen extending along the thoraco-abdominal aorta up to the iliac arteries. **3** Detail of the entry site at the level of the origin of the right renal artery, which arises from the true lumen. **4** The dissection involves both common iliac arteries

Study Protocol

Patient preparation: A 6-h fast prior to the examination; 18G intravenous catheter in the right antecubital vein.

Iodine flow rate: 2.0 gI/s.

CM concentration (mgI/mL)	Flow rate (mL/s)
300	6.7
320	6.2
350	5.7
370	5.4
400	5.0

CM volume: (Scan time + trigger delay)*flow rate.

Saline flush: 50 ml of saline at the same flow rate.

Pre-contrast scan: Unnecessary.

Post-contrast scan:
CM injection protocol: Injection time = scan time + 7-s trigger delay.
Trigger delay: 7 s after the threshold of 100 HU is reached in the ascending aorta using a bolus-tracking technique.
Scan protocol:
Gating: Retrospective or prospective (according to patient HR and technology available) to best evaluate the aortic arch.
Scan region: From the aortic arch to the pelvis.
Spiral with maximum values of pitch and thin collimation.

References

Chirillo F, Salvador L, Bacchion F et al (2007) Clinical and anatomical characteristics of subtle-discrete dissection of the ascending aorta. Am J Cardiol 15:1314-1319

Heye T, Karck M, Richter G et al (2007) Visualization of entry and re-entry tears in a complex type A aortic dissection by 64-slice dual-source computer tomography. Eur J Cardiothorac Surg 32:935

Theisen D, von Tengg-Kobligk H, Michaely H et al (2007) CT angiography of the aorta. Radiologe 47:982-992

VASCULAR – Aortic Dissection Type B

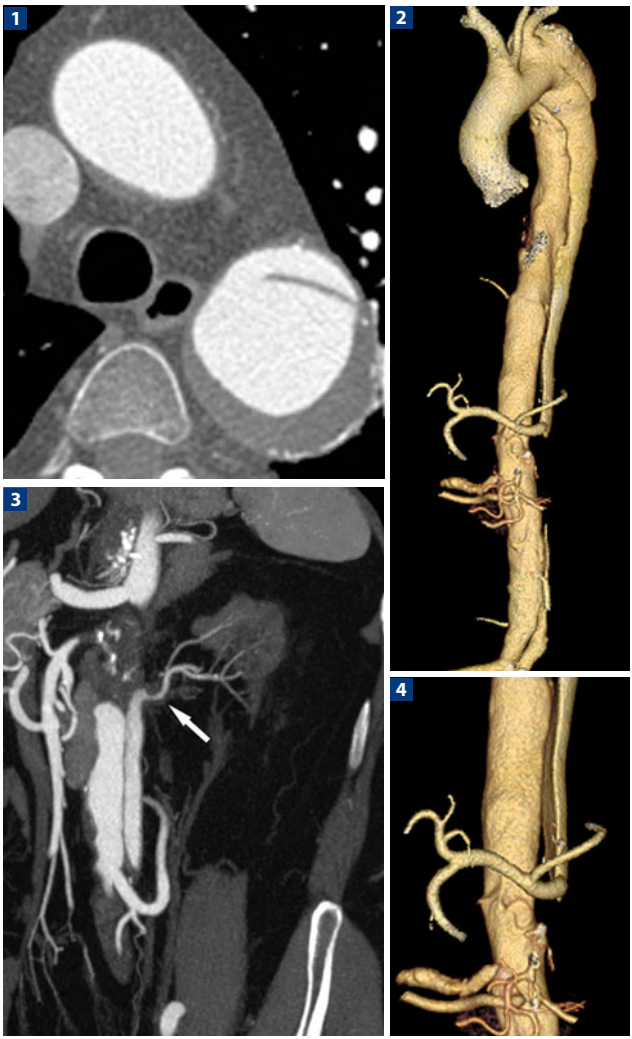

Spindle-shaped aneurysmal dilatation of the thoracic aorta after the origin of the left subclavian artery. Note the lamellar thrombotic apposition of the posterior wall and the point of entry of the intimal dissection. **1** Two-dimensional axial image. **2** VR reconstruction shows the extension of the dissection above the common iliac bifurcation. **3** On oblique MIP reconstruction, the dissection can be seen extending along the thoraco-abdominal aorta. The left renal artery arises from the false lumen (*arrow*). **4** VR reconstruction shows the origin of the left main artery from the false lumen

Study Protocol

Patient preparation: A 6-h fast prior to the examination; 18G intravenous catheter in the right antecubital vein.

Iodine flow rate: 2.0 gI/s.

CM concentration (mgI/mL)	Flow rate (mL/s)
300	6.7
320	6.2
350	5.7
370	5.4
400	5.0

CM volume: (Scan time + trigger delay)*flow rate.

Saline flush: 50 ml of saline at the same flow rate.

Pre-contrast scan: Unnecessary.

Post-contrast scan:
CM injection protocol: Injection time = scan time + 7-s trigger delay.
Trigger delay: 7s after the threshold of 100 HU is reached in the ascending aorta using a bolus-tracking technique.
Scan protocol:
Scan region: From the aortic arch to the pelvis.
Spiral with maximum values of pitch and thin collimation.

References

Mosquera VX, Marini M, Rodríguez F et al (2007) Complicated acute type B aortic dissection with involvement of an aberrant right subclavian artery and rupture of a thoracoabdominal aortic aneurysm, Crawford type I: successful emergency endovascular treatment. J Thorac Cardiovasc Surg 134:1055-1057

Romano L, Pinto A, Gagliardi N et al (2007) Multidetector-row CT evaluation of nontraumatic acute thoracic aortic syndromes. Radiol Med 112:1-20

Salvolini L, Renda P, Fiore D et al (2007) Acute aortic syndromes: role of multidetector row CT. Eur J Radiol 65:350-358

VASCULAR – Mesenteric Vessels Anomalies and Pathologic Presentations

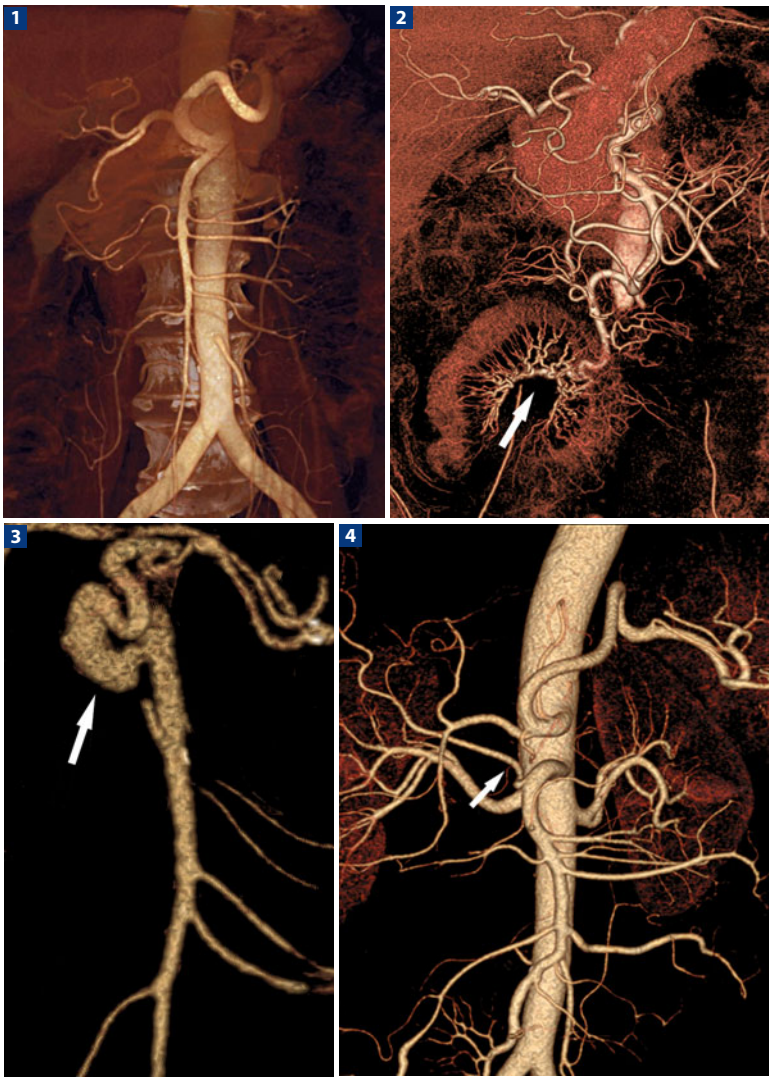

These VR reconstructions show: **1** the celiac trunk, with the common origin of the splenic artery, common hepatic artery and the superior mesenteric artery; **2** Crohn's disease, with hypertrophy of the vasa recta of the last ileal loop affected by the disease (*arrow*); **3** an aneurysm of the inferior pancreaticoduodenal artery (*arrow*); **4** the right hepatic artery arising from the superior mesenteric artery (*arrow*)

Study Protocol

Patient preparation: A 6-h fast prior to the examination; 18G intravenous catheter in an antecubital vein.

Iodine flow rate: 2.0 gI/s.

CM concentration (mgI/mL)	Flow rate (mL/s)
300	6.7
320	6.2
350	5.7
370	5.4
400	5.0

CM volume: (Scan time + trigger delay)*flow rate.

Saline flush: 50 ml of saline at the same flow rate.

Pre-contrast scan: Unnecessary.

Post-contrast scan:
CM injection protocol: Injection time= scan time + 8-s trigger delay.
Trigger delay: 8 s after the value of 100 HU is reached, with the ROI in the abdominal aorta, using a bolus-tracking technique.
Scan protocol:
Arterial phase is mandatory. The diagnostic protocol provides lower kV values (80–100 kV) with fixed mA (200 mA); alternatively automated techniques to reduce mA can be used.
Spiral with maximum values of pitch and thin collimation.
Scan region: From the diaphragmatic dome to the pelvis.

References

Capuñay C, Carrascosa P, Martín López E et al (2009) Multidetector CT angiography and virtual angioscopy of the abdomen. Abdom Imaging 34:81-93. PMID: 18709405

Ofer A, Abadi S, Nitecki S et al (2009) Multidetector CT angiography in the evaluation of acute mesenteric ischemia. Eur Radiol 19:24-30. PMID:18690454

Saba L, Mallarini G (2008) Multidetector row CT angiography in the evaluation of the hepatic artery and its anatomical variants. Clin Radiol 63:312-321

VASCULAR – Aneurysm of the Subrenal Abdominal Aorta

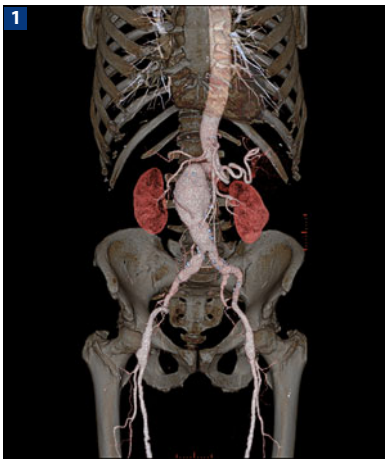

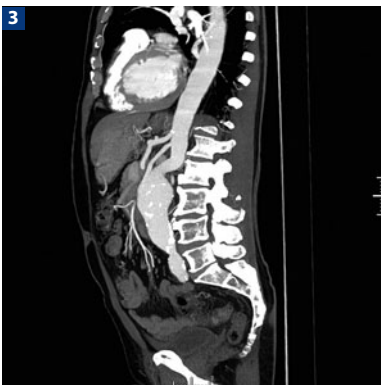

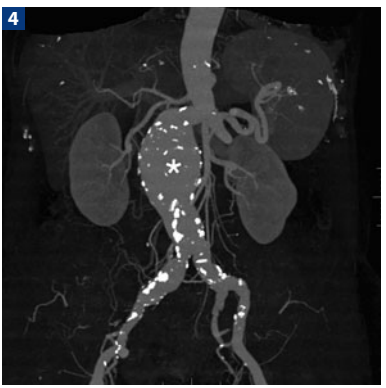

Aneurysm of the subrenal abdominal aorta with parietal thrombotic apposition. **1** VR reconstruction provides a panoramic view of a concentric aneurysm of the subrenal abdominal aorta. **2** Axial image shows the size of the aneurysm and the eccentric location of the thrombotic appositions on the anterior wall (*arrowheads*). **3**, **4** Three-dimensional sagittal and coronal MIP reconstructions demonstrate the relationships with the origin (*asterisk*) of the main splenic vessels

Study Protocol

Patient preparation: A 6-h fast prior to the examination; 18G intravenous catheter in an antecubital vein.

Iodine flow rate: 2.0 gI/s.

CM concentration (mgI/mL)	Flow rate (mL/s)
300	6.7
320	6.2
350	5.7
370	5.4
400	5.0

CM volume: (Scan time + trigger delay)*flow rate.

Saline flush: 50 ml of saline at the same flow rate.

Pre-contrast scan: Unnecessary.

Post-contrast scan:
CM injection protocol: Injection time = scan time + 8-s trigger delay.
Trigger delay: 8 s from reaching the value of 100 HU with ROI in abdominal aorta using a bolus tracking technique.
Scan protocol:
Arterial phase. The diagnostic protocol provides lower kV values (80–100 kV) with fixed mA (200 mA); alternatively, automated techniques to reduce mA can be used. Spiral with maximum values of pitch and thin collimation.
Scan region: From the diaphragmatic dome to the pelvis.

References

Albrecht T, Meyer BC (2007) MDCT angiography of peripheral arteries: technical considerations and impact on patient management. Eur Radiol 17 Suppl 6:F5-F15

Heijenbrok-Kal MH, Kock MC, Hunink MG (2007) Lower extremity arterial disease: multidetector CT angiography meta-analysis. Radiology 245:433-439

Kock MC, Dijkshoorn ML, Pattynama PM et al (2007) Multi-detector row computed tomography angiography of peripheral arterial disease. Eur Radiol 17:3208-3222

VASCULAR – Aortic Endoprosthesis with Type I Endoleak

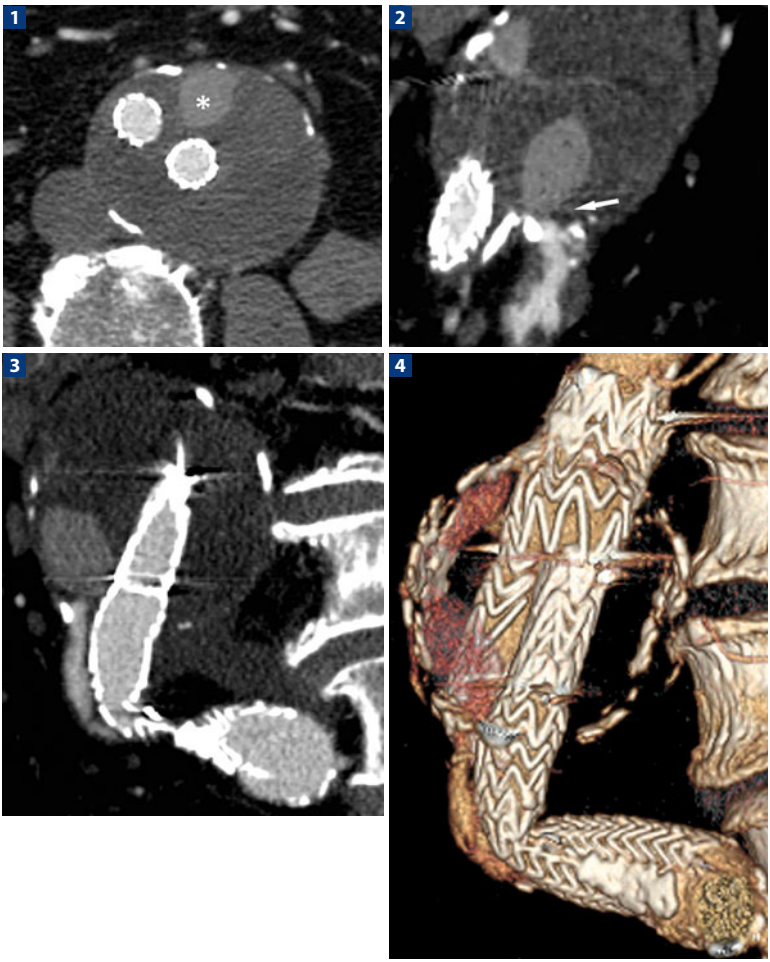

1 This 2D axial image in the arterial phase shows the bifurcated endoprosthesis with type I endoleak (*asterisk*) arising from the distal end of the left iliac arm. **2** Oblique MIP reconstruction shows the origin of the endoleak (*arrow*) at the distal end of the left iliac arm due to an ineffective seal at the end of the graft. **3** Sagittal MIP reconstruction shows the type I endoleak. Note the beam-hardening artifacts due to the metallic stent. **4** On VR reconstruction, the calcified wall of the aneurysmal sac with the presence of the endoleak can be seen

Study Protocol

Patient preparation: A 6-h fast prior to the examination; 18G intravenous catheter in an antecubital vein.

Iodine flow rate: 2.0 gI/s.

CM concentration (mgI/mL)	Flow rate (mL/s)
300	6.7
320	6.2
350	5.7
370	5.4
400	5.0

CM volume: (Scan time + trigger delay)*flow rate.

Saline flush: 50 ml of saline at the same flow rate.

Pre-contrast scan: Necessary to evaluate hyperdense components of the stent.

Post-contrast scan:
CM injection protocol: Injection time = scan time + 8-s trigger delay.
Trigger delay: 8 s after the value of 100 HU is reached, with the ROI in the abdominal aorta, using a bolus-tracking technique.
Scan protocol:
Arterial phase and a late phase with a 180-s delay to assess the late endoleak are mandatory. The diagnostic protocol provides lower kV values (80 –100 kV) with fixed mA (200 mA); alternatively, automated techniques to reduce mA can be used.
Spiral with maximum values of pitch and thin collimation.
Scan region: From the diaphragmatic dome to the pelvis.

References

Barbiero G, Baratto A, Ferro F et al (2008) Strategies of endoleak management following endoluminal treatment of abdominal aortic aneurysms in 95 patients: how, when and why. Radiol Med 113:1029-1042

Iezzi R, Cotroneo AR, Filippone A et al (2008) Multidetector-row computed tomography angiography in abdominal aortic aneurysm treated with endovascular repair: evaluation of optimal timing of delayed phase imaging for the detection of low-flow endoleaks. J Comput Assist Tomogr 32:609-615

Rydberg J, Lalka S, Johnson M et al (2004) Characterization of endoleaks by dynamic computed tomographic angiography. Am J Surg 188:538-543

VASCULAR – Aortic Endoprosthesis with Type II Endoleak

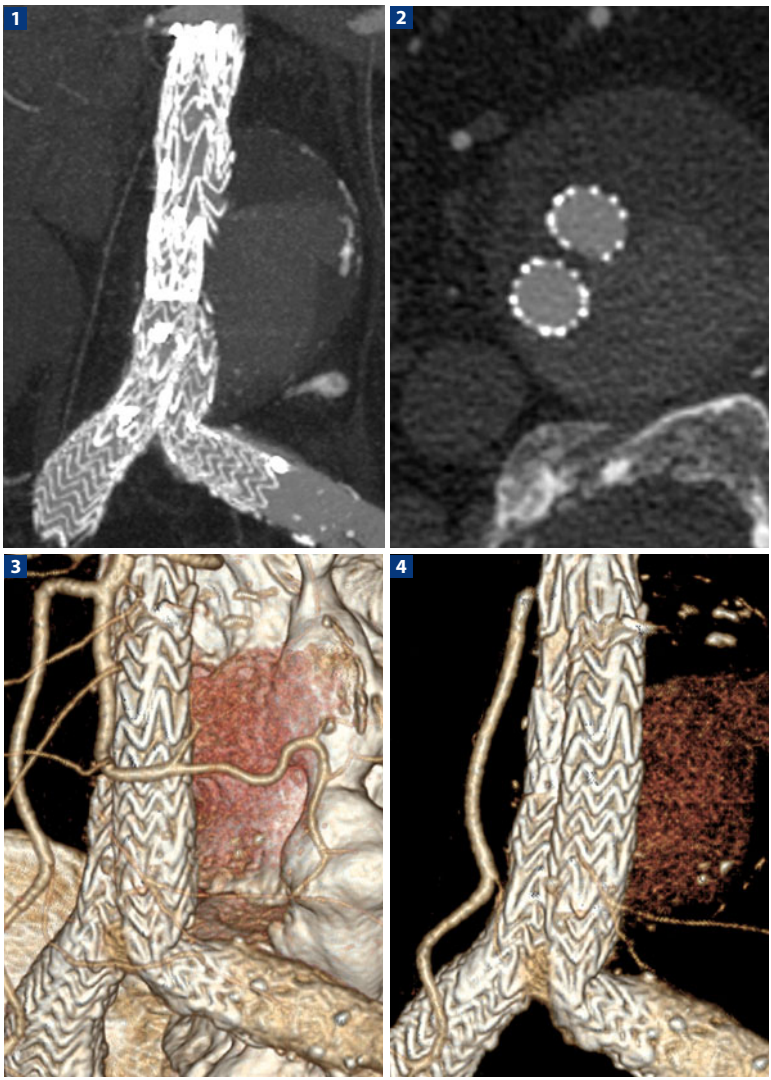

Bifurcated endoprosthesis with associated type II endoleak of the aneurysm due to refilling by the lumbar vessels. **1** Oblique MIP reconstruction. **2** The 2D axial image shows the extensive endoleak posterior to the endoprosthesis. **3**, **4** VR reconstructions: details of the endoprosthesis and the endoleak. Note the calcifications of the aneurysm

Study Protocol

Patient preparation: A 6-h fast prior to the examination; 18G intravenous catheter in an antecubital vein.

Iodine flow rate: 2.0 gI/s.

CM concentration (mgI/mL)	Flow rate (mL/s)
300	6.7
320	6.2
350	5.7
370	5.4
400	5.0

CM volume: (Scan time + trigger delay)*flow rate.

Saline flush: 50 ml of saline at the same flow rate.

Pre-contrast scan: Necessary to evaluate hyperdense components of the stent.

Post-contrast scan:
CM injection protocol: Injection time = scan time + 8-s trigger delay.
Trigger delay: 8 s after the value of 100 HU is reached, with the ROI in the abdominal aorta, using a bolus- tracking technique.
Scan protocol:
Arterial phase and a late phase with a 180-s delay to assess the late endoleak are mandatory. The diagnostic protocol provides lower kV values (80 –100 kV) with fixed mA (200 mA); alternatively, automated techniques to reduce mA can be used.
Spiral with maximum values of pitch and thin collimation.
Scan region: From the diaphragmatic dome to the pelvis.

References

Chernyak V, Rozenblit AM, Patlas M et al (2006) Type II endoleak after endoaortic graft implantation: diagnosis with helical CT arteriography. Radiology 240:885-693

Saba L, Pascalis L, Montisci R et al (2008) Diagnostic sensitivity of multidetector-row spiral computed tomography angiography in the evaluation of type-II endoleaks and their source: comparison between axial scans and reformatting techniques. Acta Radiol 49:630-637

Tolia AJ, Landis R, Lamparello P, Rosen R, Macari M (2005) Type II endoleaks after endovascular repair of abdominal aortic aneurysms: natural history. Radiology 235:683-686

VASCULAR – Aortic Endoprosthesis with Peri-prosthetic Inflammation

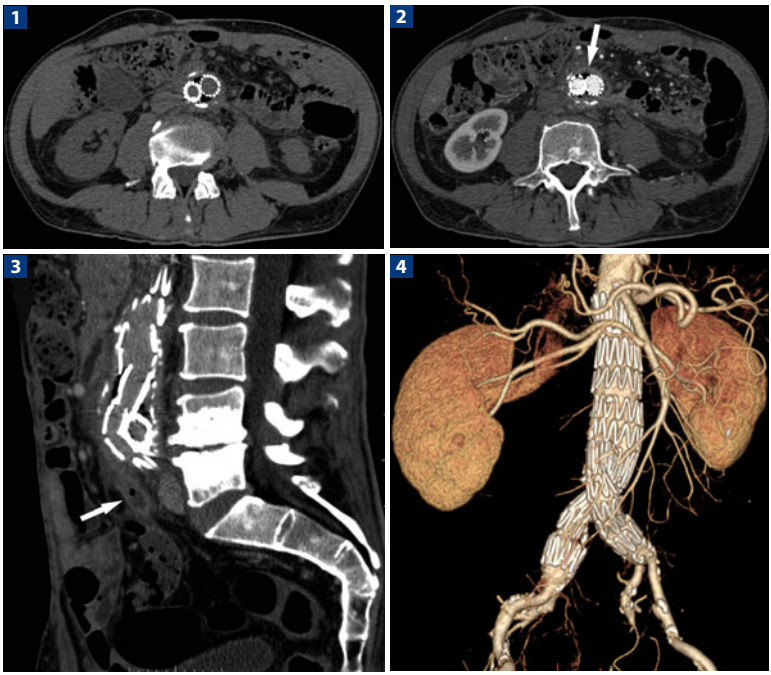

1 In this axial non-enhanced axial image, a small peri-prosthetic gaseous collection at the level of the iliac arms is already evident. **2** Contrast-enhanced 2D axial image in the arterial phase confirms the peri-prosthetic collection (*arrow*), with no signs of blood extravasation. **3** Sagittal MPR image clearly shows the peri-prosthetic collection as well as a more caudal collection (*arrow*) also probably due to abscess formation. **4** VR reconstruction: detail of the bifurcated endoprosthesis

Study Protocol

Patient preparation: A 6-h fast prior to the examination; 18G intravenous catheter in an antecubital vein.

Iodine flow rate: 2.0 gI/s.

CM concentration (mgI/mL)	Flow rate (mL/s)
300	6.7
320	6.2
350	5.7
370	5.4
400	5.0

CM volume: (Scan time + trigger delay)*flow rate.

Saline flush: 50 ml of saline at the same flow rate.

Pre-contrast scan: Necessary to evaluate hyperdense components of the stent.

Post-contrast scan:
CM injection protocol: Injection time = scan time + 8-s trigger delay.
Trigger delay: 8 s after the value of 100 HU is reached, with the ROI in the abdominal aorta, using a bolus-tracking technique.
Arterial phase and a late phase with a 180-s delay to assess the late endoleak are mandatory. The diagnostic protocol provides lower kV values (80–100 kV) with fixed mA (200 mA); alternatively, automated techniques to reduce mA can be used.
Scan protocol:
Spiral with maximum values of pitch and thin collimation.
Scan region: From the diaphragmatic dome to the pelvis.

References

Chernyak V, Rozenblit AM, Patlas M et al (2006) Type II endoleak after endoaortic graft implantation: diagnosis with helical CT arteriography. Radiology 240:885-693

Saba L, Pascalis L, Montisci R et al (2008) Diagnostic sensitivity of multidetector-row spiral computed tomography angiography in the evaluation of type-II endoleaks and their source: comparison between axial scans and reformatting techniques. Acta Radiol 49:630-637

Tolia AJ, Landis R, Lamparello P, Rosen R, Macari M (2005) Type II endoleaks after endovascular repair of abdominal aortic aneurysms: natural history. Radiology 235:683-686

VASCULAR – Celiac Trunk Stent

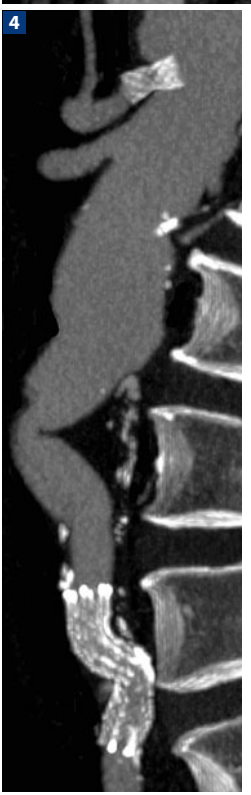

1 Two-dimensional axial image shows the presence of a stent at the level of the origin of the celiac trunk with evaluation of the trunk patency itself. **2** Two-dimensional sagittal reformatted image. **3** Detail and **4** general MIP reconstructions provide a lateral view of the stent

Study Protocol

Patient preparation: A 6-h fast prior to the examination; 18G intravenous catheter in an antecubital vein.

Iodine flow rate: 2.0 gI/s.

CM concentration (mgI/mL)	Flow rate (mL/s)
300	6.7
320	6.2
350	5.7
370	5.4
400	5.0

CM volume: (Scan time + trigger delay)*flow rate.

Saline flush: 50 ml of saline at the same flow rate.

Pre-contrast scan: Necessary to evaluate hyperdense components of the stent.

Post-contrast scan:
CM injection protocol: Injection time = scan time + 8-s trigger delay.
Trigger delay: 8 s after the value of 100 HU is reached, with the ROI in the abdominal aorta, using a bolus-tracking technique.
Scan protocol:
Arterial phase and a late phase with a 180-s delay to assess the late endoleak are mandatory. The diagnostic protocol provides lower kV values (80–100 kV) with fixed mA (200 mA); alternatively, automated techniques to reduce mA can be used.
Spiral with maximum values of pitch and thin collimation.
Scan region: From the diaphragmatic dome to the pelvis.

References

Ferrari R, De Cecco CN, Iafrate F et al (2007) Anatomical variations of the coeliac trunk and the mesenteric arteries evaluated with 64-row CT angiography. Radiol Med 112:988-998

Grierson C, Uthappa MC, Uberoi R et al (2007) Multidetector CT appearances of splanchnic arterial pathology. Clin Radiol 62:717-723

Smith CL, Horton KM, Fishman EK (2006) Mesenteric CT angiography: a discussion of techniques and selected applications. Tech Vasc Interv Radiol 9:150-155

VASCULAR – Aorto-Bifemoral Bypass

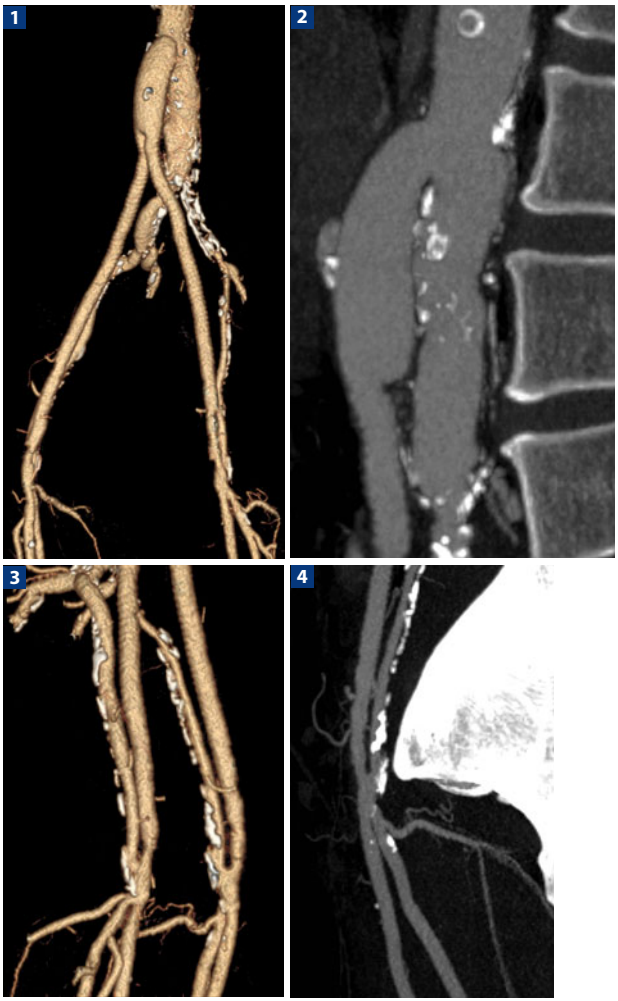

An aorto-bifemoral bypass in a patient with occlusion of the left common iliac artery and multiple fibrocalcific plaques causing significant stenosis of the right iliac axis. **1** VR reconstruction. **2** Sagittal MIP reconstruction: proximal anastomosis of the graft on the anterior wall of the subrenal aorta. **3** VR reconstruction: distal bifemoral anastomosis; in such cases, the anastomoses may be the site of occlusion such that their patency should also be evaluated. **4** Oblique MIP reconstruction shows the distal anastomosis of the left femoral artery. Note the extensive calcifications of the common femoral artery and the patency of the graft

Study Protocol

Patient preparation: A 6-h fast prior to the examination; 18G intravenous catheter in an antecubital vein.

Iodine flow rate: 2.0 gI/s.

CM concentration (mgI/mL)	Flow rate (mL/s)
300	6.7
320	6.2
350	5.7
370	5.4
400	5.0

CM volume: (Scan time + trigger delay)*flow rate.

Saline flush: 50 ml of saline at the same flow rate.

Pre-contrast scan: Unnecessary.

Post-contrast scan:
CM injection protocol: Injection time = scan time + 8-s trigger delay.
Trigger delay: 8 s after the value of 100 HU is reached, with the ROI in the abdominal aorta, using a bolus-tracking technique.
Scan protocol:
Arterial phase is mandatory. The diagnostic protocol provides lower kV values (80–100 kV) with fixed mA (200 mA); alternatively, automated techniques to reduce mA can be used.
Spiral with maximum values of pitch and thin collimation.
Scan region: From the diaphragmatic dome to the knee.

References

Fleischmann D, Hallett RL et al (2006) CT angiography of peripheral arterial disease. J Vasc Interv Radiol 17:3-26

Lopera JE, Trimmer CK, Josephs SG (2008) Multidetector CT angiography of infrainguinal arterial bypass. RadioGraphics 28:529-548

Willmann JK, Baumert B, Schertler T et al (2005) Aortoiliac and lower extremity arteries assessed with 16-detector row CT angiography: prospective comparison with digital subtraction angiography. Radiology 236:1083-1093

VASCULAR – Bifurcation Endoprosthesis and Patent Femoro-femoral Bypass

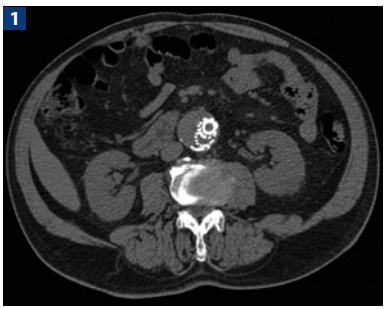

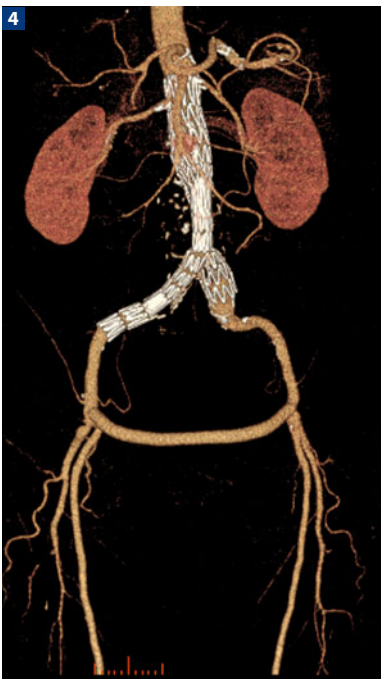

1 Non-enhanced axial image shows a bifurcated endoprosthesis with the presence of a stent in the left iliac arm of the prosthesis. **2** Axial image in the arterial phase reveals an endoleak in the anterior region of the aneurysm (*asterisk*). **3** Contrast-enhanced axial image shows complete occlusion of the left iliac arm of the prosthesis (*asterisk*). **4** Panoramic VR reconstruction shows the presence of the endoprosthesis and the patent femoro-femoral bypass

Study Protocol

Patient preparation: A 6-h fast prior to the examination; 18G intravenous catheter in an antecubital vein.

Iodine flow rate: 2.0 gI/s.

CM concentration (mgI/mL)	Flow rate (mL/s)
300	6.7
320	6.2
350	5.7
370	5.4
400	5.0

CM volume: (Scan time + trigger delay)*flow rate.

Saline flush: 50 ml of saline at the same flow rate.

Pre-contrast scan: Necessary to evaluate hyperdense components of the stent.

Post-contrast scan:
CM injection protocol: Injection time= scan time + 8-s trigger delay.
Trigger delay: 8 s after the value of 100 HU is reached, with the ROI in the abdominal aorta, using a bolus-tracking technique.
Scan protocol:
Arterial phase and a late phase with a 180-s delay to assess the late endoleak are mandatory. The diagnostic protocol provides lower kV values (80–100 kV) with fixed mA (200 mA); alternatively, automated techniques to reduce mA can be used.
Spiral with maximum values of pitch and thin collimation.
Scan region: From the diaphragmatic dome to the knee.

References

Chernyak V, Rozenblit AM, Patlas M et al (2006) Type II endoleak after endoaortic graft implantation: diagnosis with helical CT arteriography. Radiology 240:885-693

Saba L, Pascalis L, Montisci R et al (2008) Diagnostic sensitivity of multidetector-row spiral computed tomography angiography in the evaluation of type-II endoleaks and their source: comparison between axial scans and reformatting techniques. Acta Radiol 49:630-637

Tolia AJ, Landis R, Lamparello P, Rosen R, Macari M (2005) Type II endoleaks after endovascular repair of abdominal aortic aneurysms: natural history. Radiology 235:683-686

VASCULAR – Lower Limbs-Peripheral Arterial Disease

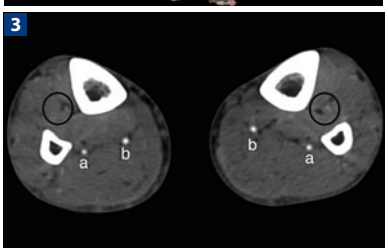

The study provides a perfect representation of the arteries of the lower limb down to the dorsalis pedis arteries. **1** Panoramic VR reconstruction with transparency of the skeletal structures. **2** Axial image at the level of the iliac bifurcation. Note the stenosis of the left common iliac artery with a not hemodynamically significant reduction in the lumen (*arrow*). **3** Axial image at the level of the arterial vessels of the lower limbs. Note the perfect representation of the interosseous (**a**) and posterior tibial (**b**) arteries, with bilateral stenosis of the anterior tibial arteries (*black circles*). **4** VR reconstruction of the vessels of the lower limbs

Study Protocol

Patient preparation: A 6-h fast prior to the examination; 18G intravenous catheter in an antecubital vein.

Iodine flow rate: 2.0 gI/s and 1.2 gI/s.

CM concentration (mgI/mL)	Flow rate (mL/s)
300	6.7/4
320	6.2/3.7
350	5.7/3.4
370	5.4/3.2
400	5.0/3

Pre-contrast scan: Unnecessary.

Post-contrast scan:
CM injection protocol:
Fixed injection time: 35 s (for patients between 60 and 90 kg).
Biphasic protocol: 1/3 of CM at 2 gI/s followed by 2/3 of CM at 1.2 gI/s every s after the threshold of 100 HU is reached in the ascending aorta using a bolus-tracking technique.
Saline flush: 50 ml of saline at the same flow rate.
Scan protocol: An arterial phase is mandatory. The diagnostic protocol provides lower kV values (80–100 kV) with fixed mA (200 mA); alternatively, automated techniques to reduce mA can be used.
Scan region: From the diaphragmatic dome to the foot.

References

Fleischmann D, Hallett RL et al (2006) CT angiography of peripheral arterial disease. J Vasc Interv Radiol 17:3-26

Lopera JE, Trimmer CK, Josephs SG (2008) Multidetector CT angiography of infrainguinal arterial bypass. Radiographics 28:529-548

Willmann JK, Baumert B, Schertler T et al (2005) Aortoiliac and lower extremity arteries assessed with 16-detector row CT angiography: prospective comparison with digital subtraction angiography. Radiology 236:1083-1093